Reactive cholangiocytes differentiate into proliferative hepatocytes with efficient DNA repair in mice with chronic liver injury

Manco, Rita; Clerbaux, Laure-Alix; Verhulst, Stefaan; Bou Nader, Myriam; Sempoux, Christine; Ambroise, Jerome; Bearzatto, Bertrand; Gala, Jean Luc; Horsmans, Yves; van Grunsven, Leo; Desdouets, Chantal; Leclercq, Isabelle

Published in:
Journal of Hepatology

DOI:
10.1016/j.jhep.2019.02.003

Publication date:
2019

Reactive cholangiocytes differentiate into proliferative hepatocytes with efficient DNA repair in mice with chronic liver injury

R. Manco[1], LA. Clerbaux[1], S. Verhulst[2], M.Bou Nader[3], C. Sempoux[4], J. Ambroise[5], B. Bearzatto[5], JL. Gala [5], Y. Horsmans[1,6], LA. van Grunsven[2], C.Desdouets[3] and IA. Leclercq[1*]

[1] *Laboratory of Hepato-gastroenterology, Institut de Recherche Expérimentale et Clinique, Université catholique de Louvain, Brussels, Belgium.*

[2] *Liver Cell Biology Laboratory, Vrije Universiteit Brussels (VUB), Brussel, Belgium.*

[3] *Inserm, U1016, Institut Cochin, Paris, France; CNRS, UMR 8104, Paris, France; Université Paris Descartes, Sorbonne Paris Cité, Paris, France.*

[4] *Institute of Pathology, Centre Hospitalier Universitaire Vaudois, Lausanne, Switzerland.*

[5] *Centre de Technologies Moléculaires Appliquées, Institut de Recherche Expérimentale et Clinique, Université catholique de Louvain, Brussels, Belgium.*

[6] *Hepato-gastroenterology Unit, Cliniques Universitaires Saint-Luc, Brussels, Belgium.*

Grant support: This work was supported by grants from the Belgian Federal Science Policy Office (Interuniversity Attraction Poles program, network P7/83-HEPRO2 and from the Fund for Scientific Medical Research (PDR T.1067.14-P) to IA.L. and from unrestricted from Gilead, Belgium.

***ADDRESS CORRESPONDENCE TO**: Isabelle Leclercq, GAEN laboratory, Avenue Mounier 53, B1.52.01, 1200 Brussels, Belgium. Phone: 32.2764.5273; E-mail: isabelle.leclercq@uclouvain.be.

COMPETING PERSONAL AND FINANCIAL INTERESTS: The authors declare no competing personal or financial interests.

AUTHORS' CONTRIBUTION: R.M. designed, conducted the experiments, analyzed and discussed the data, L-A.C. analyzed and discussed the data, S.V. and LA. vG. generated, analyzed and discussed the FACS analysis, analyzed and discussed the RNAseq data, M.B-N. and C.D. generated, analyzed and discussed the ploidy data, C.S. generated the HIC score and discussed the data, J.A., B.B. and JL Gala

analyzed and discussed the RNAseq data, Y.H. discussed the hypothesis, study design and data, I.L. designed the experiments, conducted the study, and analyzed and discussed the data; R.M. and I.L. wrote the original manuscript. All authors read and edited the manuscript.

ABSTRACT:

Chronic liver diseases are characterized by expansion of the small immature cholangiocytes – a mechanism named ductular reaction (DR) – which have the capacity to differentiate in hepatocytes. We investigated the kinetics of DR differentiation into hepatocytes as well as several important features as functional maturity, clonal expansion and resistant to stress of the newly formed hepatocytes in mice with long-term liver damage.

We track DR-cell differentiation using osteopontin-iCreER^{T2} and hepatocytes with AAV8-TBG-Cre. Mice received carbon tetrachloride (CCl_4) for >24weeks to induce chronic liver injury. Livers were collected for reporter proteins, cell proliferation and death, DNA damage, and nuclear ploidy analysis; hepatocytes were isolated for RNAseq.

During liver injury we observed a transient DR. The DR-cells differentiated into hepatocytes as clones derived from single DR-cell such as by week 8, 12% of the liver parenchyma was occupied by DR-derived hepatocytes. These hepatocytes had all features of mature functional hepatocytes. In contrast to the exhausted native hepatocytes, these newly formed hepatocytes had higher proliferation, less apoptosis, a lower proportion of highly polyploid nuclei and had better eliminated DNA damage.

In chronic liver injury, DR-cells differentiate into stress resistant hepatocytes that repopulate the liver. The process might account for the observed parenchymal reconstitution in livers of patients with advanced-stage hepatitis and can be a target for regenerative purpose.

INTRODUCTION

Persistent injury of the hepatic tissue leads to fibrosis, which eventually evolves to cirrhosis, the end-stage of any chronic liver diseases. Cirrhosis is characterized by distortion of hepatic architecture, regenerative nodules and hepatocyte dysfunction and is associated with life-threatening complications such as hepatocellular insufficiency and hepatocellular carcinoma (HCC)[1]. Liver cirrhosis is estimated to cause around 170,000 deaths annually[2]. So far, liver transplantation represents the only curative therapeutic solution for many chronic liver diseases.

In chronic liver diseases, extension of the fibrotic scars correlates with the presence of "Ductular reaction" (DR) [3,4]. This term refers to proliferation of small immature cholangiocytes, located at the most proximal branches of the biliary tree [5,6]. DR-cells (also referred to as oval cells or liver progenitor cells) express hepatocyte (CK8, CK18) and cholangiocytes (OV-6, CK7, CK19)[7–9] proteins and have the potential to differentiate into either of these two liver epithelial lineages[10]. Studies on human chronic liver diseases, including chronic viral hepatitis, auto-immune hepatitis and cirrhotic alcoholic or non-alcoholic fatty liver diseases, have highlighted substantial DR and the emergence of cells intermediate in size and immunophenotype between DR-cells and hepatocytes[3,11]. Several studies report such intermediate cells represent more than half of the hepatocyte pool in the cirrhotic liver [8,9,12]. A morphological continuum between DR, intermediate cells and hepatocytes may be interpreted as a gradual differentiation of DR in hepatocytes or as a de-differentiation of hepatocytes with acquisition of biliary traits (metaplasia). This conundrum is hard to resolve by the observation of human material. For this reason several (inducible) lineage tracing mouse strains tagging either cholangiocytes/DR cells or hepatocytes have been used in the last decade in attempt to unravel the origin, the dynamics and the fate of DR cells in various dietary, chemical or genetic rodent models of liver injury. The results of these studies remain conflicting. Studies by us and other authors, in which the fate of DR cells or hepatocytes was followed upon hepatocellular injury caused by a choline-deficient and ethionine-supplemented (CDE) diet, support the *in vivo* capability of DR to differentiate into hepatocytes, although in discrete proportion (<2,5%)[13,14,15]. Furthermore,

DR cells isolated from CDE livers largely underwent hepatocyte differentiation when transplanted *in vivo* into a compromised liver, with an improvement of both liver architecture and function[16]. In zebrafish the biliary compartment is also capable of generating functional hepatocytes[17]. On the other hand, studies using the 3,5-diethoxycarbonyl-1,4-dihydrocollidine (DDC) diet as model of cholangiocytic injury failed to demonstrate DR contribution to the hepatocyte pool[18-19] and other works even support a de-differentiation of traced hepatocytes into biliary-like cells[20–22]. Taken together such inconsistent data indicates that the involvement of DR cells in regeneration is conditioned by the epithelial compartment undergoing damage and is thus disease-specific; while considerable discrepancies between models and observations in human material may stem from fundamental differences in severity and chronicity of injury. Here, we aimed to analyze DR and its contribution to regeneration in a model replicating chronicity, severity and fibrotic progression seen in chronic hepatitis in humans.

Impaired hepatocyte proliferative capacity is the essential requirement for DR[23]. Recently, the capacity of the DR cells to maintain the liver parenchyma was demonstrated using genetic approaches to delete *Mdm2*[16], to provoke p53-mediated senescence in all the hepatocytes, or β1-integrin[24] to inhibit hepatic growth factor signaling thereby precluding hepatocyte replication, or β-catenin directly in the hepatocytes to impair their proliferation[25]. Such genetic models artificially cause subacute hepatocyte failure, as opposed to progressive lesions occurring during chronic liver injury. Deng et al. demonstrated thus the capability of the DR cells to differentiate into hepatocytes in a long term injury model (up to 52 weeks) using the thioacetamide (TAA) toxicant agent[26]. However, the kinetics of the response to the injury as well as several features of the DR-derived hepatocytes, such as level of maturation, clonal expansion and resistant to stress remains unanswered.

Here, we used a model of chronic liver injury mimicking in evolution and severity chronic human diseases and followed the fate of DR cells, evaluating their contribution to the pool of hepatocyte

and to characterize the newly formed hepatocytes. We show that DR emerges from clonal expansion of cholangiocytes; DR cells then undergo hepatocyte differentiation and clonal proliferation. Data were confirmed using a hepatocytes tracing lineage. The mature and functional newly formed hepatocytes have a survival, proliferative and DNA repair advantage that favors their amplification over native hepatocytes (i.e. those arising from division of pre-existent hepatocytes).

METHODS

Animal Models

To follow the fate of biliary/DR cells we used Osteopontin-iCreER^{T2} (OPN-Cre) mice crossed with Rosa26R^{YFP} [27], Rosa26R$^{mT/mG}$ [28] or Rosa26R^{Confetti} [29]. To achieve *Cre-LoxP* recombination, tamoxifen (T5648; Sigma) at a concentration of 30 mg/ml corn oil was injected i.p. at 100 mg/kg BW for 2 consecutive days on 21 and 23 days old OPN-Cre;Rosa26R^{YFP} and OPN-Cre;Rosa26R$^{mT/mG}$ mice or at 175 mg/kg BW for 5 days to ≥ 40gr OPN-Cre; Rosa26R^{Confetti} mice[30]. To genetically label the hepatocytes, AAV8-TBG-Cre adenovirus was injected i.v. at a concentration of 7, $5*10^{11}$ gc/mouse in Rosa26R^{YFP} or Rosa26R$^{mT/mG}$ reporter mice[31]. We used YFP IHC or direct observation under the fluorescence microscope to analyze tagged cells, respectively (see Suppl. Information). One month after tamoxifen treatment (to ensure complete tamoxifen wash-out) chronic liver injury was induced by repeated intraperitoneal injection of carbon tetrachloride (CCl_4) 3 times per week for 4, 6, 8, 16 and 24 weeks. Starting dose of CCl_4 was of 500 µl/kg, with dose increase up to 800 µl/kg when animals gained weight. Liver were analyzed 72h after the last CCl_4 injections or after a 2 or a 4 weeks CCl_4-free recovery period. Transgenic mice that did not receive tamoxifen were used as controls. The size of the groups is specified in the figure legends.

Mice were housed at 4-5/cage, maintained at a constant temperature of 22°C, exposed at all times to a 12-h light/12-h dark cycle and had access to food and water *ad libitum.* Animal care was provided in accordance to the guidelines for humane care for laboratory animals in accordance with European regulations and in conformity with ARRIVE guidelines. The study protocol was approved by the university ethics committee for the use of experimental animals.

FACS sorting analysis

Livers from control OPN-Cre;Rosa26R$^{mT/mG}$ mice were dissociated using pronase and collagenase to obtain a single cell suspension[32]. Two centrifugations of 50g were performed to separate the non-parenchymal fraction from the hepatocytes. We blocked the non-parenchymal fraction using bovine

serum albumin for 10 min and incubated cells with the indicated antibodies for 15 min. After adding propidium iodide we used a FACSAriaII (BD) to isolate LSECs ($CD32^+F4/80^-UV^-PI^-$), macrophages ($F4/80^+CD32^-UV^-PI^-$), HSCs ($UV^+F4/80^-CD32^-PI^-$) and BECs ($EpCAM^+UV^-CD45^-PI^-$). Hepatocytes were resuspended in PBS and immediately sorted. In each population cells were analysed for tdTomato (red) and mGFP (green) fluorescence.

For the isolation of hepatocytes for RNA sequencing, livers from TAM-injected untreated and CCl_4 treated OPN-Cre;$Rosa26R^{mT/mG}$ mice were digested using a two-step collagenase method. Solutions were perfused through the portal vein. Two centrifugations of 50g were performed to separate the non-parenchymal cells from the hepatocytes. The resulting hepatocyte populations were filtered through a 100µm filter and resuspended in 2mM EDTA + 1% FBS solution and sorted by a FACSAriaIII (BD) according to the presence of mTomato and mGFP fluorescence. Dead cells were excluded by ToPro3 staining. Sorted cells where lysed and the RNA was extracted using Qiagen RNeasy Mini kit (Promega) and processed for RNA sequencing.

Polyploidy analysis

Immunostained liver sections (β-catenin/YFP/Hoechst) were imaged with a nanozoomer 2.0, Hamamatsu fluorescent microscope associated with image management software NDP view. For ploidy analysis, Hoechst labelling was used to recognize hepatocytes nuclei with a roundness >0.8. Nuclear area was detected automatically by a specific macro developed with ImageJ software (pixels ranging from 200 to 2,500 px2). For each animal analyzed, more than 10000 nuclei were counted.

IHC score of liver tumors

Consecutive liver sections stained for ck19, GS, β-catenin and Ki67 were scored by the expert pathologist Dr. Christine Sempoux. Nodules with a diameter >1.5 mm were selected and evaluated as follow: GS was classified as normal (0) when expressed around the central vein or aberrant (1) if the expression was diffuse in the nodule or completely lost; β-catenin was evaluated as normal (1),

cytoplasmatic (2) or cytoplasmatic/nuclear (3); ki67 was classified as less than 10% (1), 10-25% (2) or more than 25% (3) level. None of the nodules expressed ck19.

Additional information on methods (carcinogenetic animal model, qPCR analysis, immunohistochemistry, RNAsequencing) is provided in supplementary document.

RESULTS

DR cells differentiate into hepatocytes, contributing significantly to the liver parenchyma.

Mice were repeatedly injected with CCl_4 for up to 16 weeks (Fig. 1a) to induce repeated cycles of central necrosis and wound healing leading to progressive fibrosis. Sirius red staining revealed central bridging fibrosis after 4 weeks, extension and thickening of fibrotic bundles progressively increased with time (Fig. 1b).

During the injury, we followed the fate of biliary/DR cells using tamoxifen-inducible osteopontin-i*CreER*^{T2} (OPN-Cre) mice crossed with Rosa26R^{YFP} or with Rosa26R$^{mT/mG}$ reporter mice to label biliary cells. Activation of the OPN promoter in cholangiocytes drives the expression of the inducible Cre recombinase. Tamoxifen binds the mutated estrogen receptor ER^{T2} and allows the activation and the translocation of the Cre-recombinase into the nucleus. Nuclear Cre-recombinase was only found in biliary OPN^{+} cells in tamoxifen-injected OPN-Cre;Rosa26R^{YFP} mice but not in mice that did not receive Tamoxifen (Suppl. Fig 1a). Recombination of the *Rosa26R* locus ensued and, according to the reporter strain, caused permanent expression of yellow fluorescent protein (YFP) in >85% of the cells of the biliary compartment or switched the expression of mTomato to that of mGFP in OPN-expressing cells with a 60% efficiency (suppl. Fig. 1b-d). No YFP^{+} or mGFP^{+} cells have been observed in livers harvested from tamoxifen-free OPN-Cre;Rosa26R^{YFP} or OPN-Cre;Rosa26R$^{mT/mG}$ mice, respectively (Suppl. Fig. 1b; not shown). As reported by us[13,31] and others[33] and verified here again by cell sorting in tamoxifen treated OPN-Cre;Rosa26R$^{mT/mG}$ mice (Suppl. Fig. 1c and Suppl. Fig. 2) upon

tamoxifen injection reporter gene expression is restricted to the biliary compartment and does not occur in hepatocytes, stellate cells, liver sinusoidal endothelial cells or Kupffer cells.

With this system, in the course of CCl_4 treatment, any YFP^+ hepatocyte would sign its biliary origin. After 4 weeks of tamoxifen wash-out, mice were treated with CCl_4. After 4 weeks of CCl_4, rare YFP^+ hepatocyte-like cells were observed in the vicinity of DR (Fig. 1c). As duration of liver insult increased, the number of YFP^+ hepatocytes raised to reach a maximum at the 8 weeks' time-point, such as 12% of the liver parenchyma was occupied by DR-derived hepatocytes (Fig. 1c-d). By contrast, in tamoxifen-free OPN-Cre;$Rosa26R^{YFP}$ mice, no YFP^+ cells and in particular no YFP^+ hepatocytes where found in the course of CCl_4 treatment (Suppl. Fig. 3). Thus, DR cells give rise to hepatocyte-like cells during chronic wound healing, supporting results showed in previous study[26]. The emergence of YFP^+ hepatocytes-like cells after 6wks CCl_4 coincided with a marked drop in proliferative activity of native hepatocytes as assessed by Ki67 index (Fig. 1e and Suppl. Fig. 4), as well as with an increased expression of p16 and p21 senescence markers and of the checkpoint kinases 1 (CHK1) and 2 (CHK2) (Fig. 1g). The YFP^+ hepatocytes formed patches, which size increased with disease progression (Fig. 1c-f). After 6 weeks, a majority (>70%) of clusters were composed of 2-3 YFP^+ hepatocyte-like cells. Over time, the proportion of small clusters declined while that of larger ones increased (Fig. 1f). The YFP^+ hepatocytes were HNF4α positive (Fig. 2a) and expressed hepato-specific liver enzymes according to their lobular location, such as expression of GS and CYP2E1 when pericentral or of CPS1 when periportal (Fig. 2b-c). Ceacam1 staining confirmed that YFP^+ hepatocytes were polarized and formed bile canaliculi with adjacent hepatocytes whether YFP^+ or YFP^- (Fig. 2d). Also, YFP^+ cells stored glycogen similarly to native YFP^- hepatocytes (Fig. 2e). They did however not express biliary markers, such as ck19, the antigen epithelial cell adhesion molecule (EpCAM) or the cholangiocyte factor HNF1β (Suppl. Fig.5). We isolated native ($mTomato^+$) and DR-derived ($mGFP^+$) hepatocytes from OPN-Cre;$Rosa26R^{mT/mG}$ after 16wks CCl_4 (Fig. 2f; suppl. Fig 6) and compared their transcriptome by RNAseq analysis. Healthy $mTomato^+$ hepatocytes from untreated OPN-Cre;$Rosa26R^{mT/mG}$ served as controls (Fig. 2f). In the 3 populations, there was a similar high count of

hepatospecific genes such as albumin (Alb), Transthyretin (Ttr) and Cyp7a1. (Fig. 2g). They also had similar expression of Cyp2E1 and Glutamine Synthetase (Glul) (Suppl. Fig. 7d).

To confirm that the new hepatocytes do not come from the division of pre-existing hepatocytes in the CCl_4 injury model[34], we performed an independent mirror-experiment in which hepatocytes' fate was analysed. Injection of AAV8-TBG-Cre adeno-associated virus to $Rosa26R^{YFP}$ mice induced YFP expression in nearly 100% of hepatocytes and zero cholangiocytes or non-parenchymal cells (Suppl. Fig. 8). Following chronic CCl_4 injections (Suppl. Fig. 9a), patches of unlabelled $HNF4\alpha^+$ and $ck19^-$ hepatocytes emerged in the liver (Fig 3a-b). Their size grew with duration injury comparably to the patches of DR-derived hepatocytes traces using the $OPN\text{-}CreER^{T2}$;$Rosa26^{YFP}$ system (Fig 3c).This confirms the emergence of clusters of hepatocytes not derived from division of pre-existing labelled hepatocytes.

Long term CCl_4 induces a discrete and transient Ductular Reaction.

We then evaluated the kinetics of the DR response. $Ck19^+$ bile ducts, normal in number and in morphology, were present in controls as well as diseased livers. After 4 and 6 weeks CCl_4, in addition to normal bile ducts, discrete DR appeared as strings of $ck19^+$ small cells irradiating the parenchymal lobule from the portal tract (Fig. 4a-b). Interestingly, in livers treated for longer duration (8-16 weeks), although the DR-derived hepatocytes increased in number (Fig. 1c-d), $ck19^+$ cells were limited to bile ducts and no DR was observed (Fig.4a-b). The expression of Sox9 (a biliary transcription factor)[35], Fn14 (a cell membrane receptor that transduces mitogenic signals to DR cells)[36], Epcam and NCAM (cell adhesion molecules highly expressed in DR)[37], all genes expressed explicitly in cholangiocytes but not in hepatocytes (Suppl. Fig. 10), confirmed the transient activation of a ductular response during CCl_4 course (Fig. 4c). In keeping, expression of genes related to the Notch pathway (Notch1, Notch2, Jagged1, Hey-1), which activation is required for biliary specification[10], were concordantly expressed at higher levels in 6 weeks CCl_4 livers but no longer at later time-points (Fig. 4d).

DR cells clonally expand and differentiate into hepatocytes with a proliferative advantage.

Our observations of transient DR and of progressive rise in the size of DR-derived hepatocytes clusters suggest that few or single biliary cells expand as DR and undergo hepatocyte differentiation followed by several rounds of cell division. To test this hypothesis, we used the OPN-Cre;Rosa26R^{Confetti} mice[29] in which tamoxifen injections results in stochastic expression of one of the four fluorescent proteins (nGFP, mCFP, RFP and YFP) encoded in the confetti allele in the OPN^{+} biliary cells. In control uninjured livers, 15-20% of cholangiocytes of the bile ducts were labelled by one of the 4 fluorescent proteins (Suppl. Fig 11). After CCl_4, all cells in a given DR expressed the same fluorescent protein (Fig. 5a), and not a mosaicism of different fluorescent proteins or of tagged/untagged cells. This observation supports that DR emerges from clonal expansion of one single biliary cell.

Also, all DR-derived hepatocytes within a patch were found to express a same one fluorescent protein (Fig. 5b). No mosaicism with a different fluorescent protein or with unlabelled hepatocytes was found into such patches. The dimension of the patches was similar to the dimension of those observed when using the Rosa26R^{YFP} reporter mice (Suppl. Fig. 11b).

As also shown above in OPN-Cre;Rosa26R^{YFP} livers (Fig. 1-3), the number of tagged hepatocytes in patches is larger than the number of cells in the original DR supporting that during chronic liver injury, biliary cells undergo clonal proliferation as DR, then transformed into hepatocytes; the number of which subsequently increases due to several rounds of cell division.

If clonal expansion of differentiated hepatocytes support patches growth, we should observe transition features between DR cells and hepatocytes in nascent patches but not anymore at later stages. We measured thus the size of hepatocytes. Coherently, we found that DR-derived cells were significantly smaller than adjacent native hepatocytes at the early 6 week time-point but at 16 weeks they were as large as native hepatocytes (Fig. 5c). Size of hepatocyte was also measured in the AAV8-TBG-Cre X Rosa26R^{YFP} mice confirming the increase in size of unlabelled (non-hepatocyte origin) cells with the progression of the injury (Suppl. Fig. 9b). DR-derived hepatocytes had a higher

proliferation index (% of $Ki67^+$ cells) (Fig. 5d), a higher percentage of cells expressing cyclin D1 (Suppl. Fig. 12) or engaged in mitosis (phospho Histone-H3 positive) (Fig. 5e) compared with native hepatocytes, further support that proliferation of differentiated mature cells contribute to growth of DR-derived hepatocytes patches

DR-derived hepatocytes better response to stress signals.

YFP^+ hepatocytes when located in the pericentral area (representing 10% of the YFP^+ hepatocytes contingent - Suppl. Fig.7a) express CYP2E1 (Fig. 2c). Moreover, CYP2E1 and GS were similarly expressed at the same level in the DR-derived and native hepatocyte populations (Suppl. Fig. 7d). We therefore assumed that a similar proportion of the 2 cell populations are able to metabolize CCl_4 and undergo CCl_4-induced damage. To study the cells' response to DNA damage, we checked the expression of genes involved in the DNA repair machinery in native (mTomato-Red) and DR-derived (mGFP-Green) injured hepatocytes, sorted after 6 and 8 weeks CCl_4, and compared them with healthy control hepatocytes. The expression of BRCA1, RAD51 and FANCI (encoding for proteins that bind DNA damage site), expression of the gatekeeper GADD45 as well as of the checkpoint kinases 1 and 2 (CHK1/2) were similarly increased in the 2 populations of native and DR-derived injured hepatocytes compared to the healthy control hepatocytes (Fig. 6a). Moreover, upon CCl_4 exposure, a similar proportion of cells of the YFP^+ and YFP^- population harbour nuclear γH2AX, a protein that aggregates to DNA breaks (Fig.6b). The proportion of $TUNEL^+$ apoptotic cells was however lower in DR-derived than in native hepatocyte population (Fig. 6c). Consistently, analysis from RNAseq data confirming that native population was enriched in the pathways involved in the regulation of DNA damage, apoptotic process and senescence (Fig. 6d).

Polyploidy, a feature of mature hepatocytes[38], is determined by the number of nuclei per cell (cellular polyploidy) and the DNA content for each nucleus (nuclear polyploidy). During liver development, polyploidization is mostly associated with modification of cellular polyploidy[39] whereas under stress condition nuclear polyploidy is altered[40]. Thus, in our context of CCl_4

treatment, we have focused on nuclear polyploidy analysis. Compared to untreated controls, YFP^- native hepatocytes display lower proportion of tetraploid nuclei (4n), and a higher proportion of highly polyploid nuclei (≥8n) as expected under CCl_4 stress condition. By contrast, YFP^+ nuclei showed a similar polyploidy profile than untreated livers with a low proportion of highly polyploid nuclei (≥8n) (Fig. 6e). All these results suggest that although native and DR-derived hepatocytes similarly experience DNA damage in ongoing CCl_4-injury, DR-derived hepatocytes have a survival advantage over native hepatocytes with less cells driven into death or senescence.

DR-derived hepatocytes have a proliferative and DNA repair advantage upon recovery.

Thus, newly formed DR-derived hepatocytes have less stress stigmata (and are potentially genetically more stable) and the balance proliferation/death favours their amplification over native hepatocytes. To verify the repopulation advantage of YFP^+ DR-derived cells, we exposed the mice to 16 wks CCl_4 and allowed the liver to recover for 2 or 4 weeks. The parenchymal area occupied by YFP^+ hepatocytes increased from 4.5% after 16 weeks CCl_4 to 7.5% and up to 13.5% after 2 and 4 weeks recovery, respectively (Fig. 7a-b). The increase in the number of YFP^+ hepatocytes was explained by an increase in the size of YFP^+ clusters (Fig. 7c) and not by the number of clusters (not shown) or the cellular size (Fig. 7d). Although the total number of $ki67^+$ cells decreased during recovery (Suppl. Fig. 13), the proliferative index (Fig. 7e-f) and the number of $pHH3^+$ mitotic cells (Fig. 7g) was higher in YFP^+ than in YFP^- hepatocytes upon recovery. γ-H2AX accumulates to form foci on damaged DNA to recruit DNA repair by homologous recombination upon injury. Indeed, as mentioned above (Fig. 6b) and as it is shown in Fig. 7h, the 2 populations of hepatocytes upon injury similarly accumulated nuclear γH2AX. Persistence of nuclear γ–H2AX foci once injury has resolved signs the presence of unrepaired DNA[41]. Native hepatocyte retained nuclear γ–H2AX protein upon recovery while it was rapidly cleaned in YFP^+ hepatocytes (Fig. 7h and Suppl. Fig. 14). Collectively, these data support the concept that the increased number of DR-derived hepatocytes upon recovery from injury is achieved by effective proliferation of unstressed cells previously differentiated from

DR, while YFP$^-$ native hepatocytes harbour unrepaired DNA damage and are significantly less replicative.

DR-derived hepatocytes are not involved in the development of pre-neoplastic nodules.

The cirrhotic liver is a precancerous organ. Twenty-four weeks of CCl_4 caused macronodular cirrhosis (Fig. 8a-b). Although YFP staining revealed some cirrhotic nodules entirely composed by YFP$^+$ cells or mosaic YFP$^+$/YFP$^-$ (arrows in Fig. 6B), the majority of nodules were nonetheless YFP$^-$ (Fig. 8c). Glutamine synthetase (GS) expression, a proxy for β-catenin activation described in preneoplastic lesions and a useful marker to identify neoplasia[42], was found in 40% of YFP$^-$ nodules and only in 10% of YFP$^+$ regenerative nodules (Fig. 8d-e). Moreover, in mosaic YFP$^+$/YFP$^-$ nodules, GS expression was restricted to YFP$^-$ area while YFP$^+$ DR-derived hepatocytes did not express GS (insert Fig. 6d). Compared to normal hepatocytes in the undamaged liver, YFP$^-$ native hepatocyte nuclei were more often highly polyploid (>8n) and more rarely tetraploid (4n) in the cirrhotic liver (Fig. 8f). By contrast, the level of nuclear polyploidy of DR-derived YFP$^+$ hepatocytes in the cirrhotic liver was comparable to that of hepatocytes in an undamaged liver (Fig. 8f) suggesting, also at this stage of the disease, a higher protection or a better capacity of DR-derived YFP$^+$ cells to manage stress induced by CCl_4 treatment. Similar to Tummala *et al.*[43], we applied to regenerative nodules a composite index based on immuno-detection of GS, β-catenin and Ki67 (IHC score) for diagnosis of malignant hepatocellular neoplasms. The index was low in all cirrhotic nodules compared to score in proven HCC[31] taken as reference (Suppl. Fig. 17d) but notably the YFP$^+$ nodules had a lower score than the YFP$^-$ nodules (Fig. 8g). Then, we interrogated the susceptibility of native and DR-derived hepatocytes to carcinogenesis, using the carcinogenic agent DEN (Suppl. Fig. 15a). Out of 15 mice, 12 developed macroscopic tumours. Altogether, 26 nodules were diagnosed as HCC (Suppl. Fig. 17). They were, however, all YFP$^-$ and no YFP$^+$ HCC were found.

DISCUSSION

It is now established from recent studies that cells from the biliary compartment give rise by proliferation to the ductular reaction and by cell differentiation to functional hepatocytes[15,24,26]. The latter has been demonstrated in models in which hepatocellular injury associates with genetic abrogation of their replicative capacity[15,24,25] as well as in long term TAA-injury model[26]. However, the kinetics of cell differentiation from a biliary precursor and characterization of the new hepatocytes have not up to now been investigated.

The present study was designed to test the efficiency and safety of this alternative regeneration pathway in a model of chronic hepatocellular disease. We used a model of repeated administration of the hepatotoxic CCl_4 to induce repeated rounds of parenchymal necrosis and healing that culminate to cirrhosis, mimicking in its evolution and severity chronic liver injury in humans. The use of efficient and clean genetic tracing of cholangiocytes[33] or conversely of native hepatocytes enables to monitor the relation between the ductular reaction and generation of hepatocytes from DR cells compartment at various stages of disease progression. With these tools, our experiments confirm unambiguously that DR yield ~12% of hepatocytes in the chronically ill liver. Our results are in conflict with most of the previous papers[14,30,44], including previous work of the lab[13] in which the fate of DR and transit amplifying cells was traced in CCl_4 experiments. The discrepancy results from the experimental protocol and whether it impedes hepatocyte regeneration. We followed the scheme already published by our lab: 3 injections of CCl_4 per week with adaptation of the dose to the body weight. 4 weeks of CCl_4, as in Español-Suner et al[1313], caused a discrete DR and no DR-derived hepatocytes were observed. In the others papers in which the expression "chronic CCl_4" was used, CCl_4 was administrated only twice a week, for 5, 6 or 8 weeks[14,30,44]. None of those papers reported the hepatocytes proliferation, but we can speculate that the dose and timing of the CCl_4 injections were not enough to inhibit hepatocytes proliferation. As evidence for this hypothesis, Pu et al. reported that the periportal Mfsd2a$^+$ native hepatocytes repopulate the liver lobules during "chronic" CCl_4, confirming that they are not in a state of replicative senescence[34].

Similar to our data, Deng et al. recently published the contribution of cholangiocytes to parenchymal regeneration in a model of long lasting TAA-induced liver disease[26]. However, in the TAA model both native and cholangiocyte-derived hepatocytes had similar proliferation as far as assessed by ki67 analysis, leaving the mechanism for rising proportion of cholangiocytes-derived hepatocytes at this time unexplained. Coherent with our data, the same authors reported using the AAV8-TBG-Cre;mTmG system, that after long term (24weeks) TAA insult 2 $mTom^+$ hepatocytes composed 20% of the parenchyma, i.e. that these 20% of the hepatocytes did not derived from proliferation of native $mGFP^+$ (and $mTom^-$) hepatocytes. In the same model, 7% of the hepatocytes were demonstrated to be of biliary origin. The difference in number might be ascribed to the relatively poor efficiency of biliary labelling in ck19-CreER mice (70%). By using a similar approach but a much more efficient system to trace biliary cells (>85% efficiency), the patches of hepatocytes that appear after long term CCl_4 in our study were similar in size whether traced as of DR-origin or, in the mirror experiment, as of non-hepatocytic origin.

In addition, we studied the temporal evolution of the DR-differentiation process, found that in CCl_4-induced injury, DR stems from clonal amplification of a discrete population of biliary cells, the identity of which remaining to be ascertained. Thereafter DR cells, or a subset of them undergo complete hepatocytic differentiation yielding functional cells, perfectly organised within the lobular architecture (Fig. 3). Coherently with studies by Lu[16] and Raven[24], initial differentiation of DR cells into hepatocytes coincided with the injury-induced drop in replication of native hepatocytes. Morphometric analyses revealed that early in the process, newly differentiated hepatocytes are small in size and reach a normal size with time while they amplify. Clonality experiments in confetti mice highlight that all DR-derived hepatocytes within a patch harbour one and unique fluorescent tag, identical to that expressed by adjacent DR cells signing genetic filiation. Yet when hepatocyte patches expand, DR vanishes. These data suggest that during chronic liver injury, DR does not constantly re-fuel the parenchyma with newly differentiated cells, but rather when sufficient and appropriate cellular and environmental conditions are met, a limited contingent of DR cells undergo

differentiation then clonal expansion to repopulate up to 12% of the liver. Further studies will be needed to determine whether the subset of DR cells could correspond to $ST1^{hi}$ clonogenic cholangiocytes[45], or $Lgr5^{+}$ liver stem cells[46], or the peripheral ductule described by Kamimoto et al.[6]. Pulse labelling of DR cells during disease progression would be required to test this hypothesis[6].

Our experimental system also permits to analyse separately the properties and contribution to regeneration of hepatocytes newly generated from DR cells and native hepatocytes, i.e. those already present before injury. At all times in the process, proliferative and mitotic indices are higher in the newly emerged population of hepatocytes than in native hepatocytes. Cell death by apoptosis and senescence is conversely less frequent in DR-derived hepatocytes that in adjacent native hepatocytes during chronic exposure to CCl_4 supporting that the former have a proliferative advantage over native hepatocytes. These findings suggest an explanation for sometimes extensive parenchymal reconstitution in advanced stage chronic viral hepatitis in humans[9] that has not been convincingly demonstrated in acute or mild human hepatitic injury or in most animal models of human disease. As native hepatocytes eventually become damaged and consequently senescent, the DR-derived hepatocytes then begin to repopulate owing to their untapped replicative potential[9]. This proposal was further supported by a higher proliferation rate of the DR-derived population once the injurious toxic was retrieved resulting in a significant proportional increase in the lobular area occupied by DR-derived hepatocytes and hence a decreased proportion of native hepatocytes in the lobules. As a result, DR contribute to the regeneration of a significant proportion of the parenchyma in the chronically injured liver.

The ploidy pattern of DR-derived and native hepatocytes also differed. As reported elsewhere[40] various stress signals, among which oxidative stress, provoke a decrease in the proportion of stable tetraploid nuclei and a rise in that of highly polyploid nuclei. In a context of CCl_4 treatment, we observed this precise stress-induced shift in native hepatocytes but not in DR-derived hepatocytes. Indeed, the latter, although being exposed to CCl_4 and appropriately expressing CYP2E1 necessary for CCl_4 activation, exhibited a nuclear polyploid pattern similar to that of liver parenchymal cells in

an unarmed liver. This differential ploidy pattern persisted despite continuation of CCl_4 administration. By maintaining a less polyploid genome, DR-derived hepatocytes would, like stem cells do, retain a higher replicative potential with a lower risk to accumulate DNA damage. In support to this, DR-derived hepatocytes in the healing liver retained less γ–H2AX foci and thus unrepaired DNA. Moreover, when exposed to DEN, a carcinogenic agent, native but not DR-derived hepatocytes underwent carcinogenic transformation, supporting stress resistance and stability of the latest. Whether indeed DR-driven regeneration reduces the risk of cancer would need to be confirmed in dedicated studies.

We provide here evidence that DR-derived hepatocytes represent a population of younger and healthier hepatocytes into an injured liver. Stimulation of DR-derived regeneration *in vivo* appears therefore as a safe strategy to alleviate liver insufficiency in chronic liver disease. However, several key issues are awaiting answers. Our experimental design does not allow identifying the characteristics empowering (a subset of) biliary cells with reactive capacity to mount the ductular reaction (the "target cells" for DR-derived regeneration). They could correspond to the label retaining cells recently described by Cao et al[47]. Also, while failure of mature hepatocyte to divide and regenerate the organ contributes to trigger DR and its differentiation, many other processes activated during wound repair are likely to be involved such as vascular changes, inflammation, modification of the ECM scaffold, *etc*[8,12,48]. Whether all small DR-derived hepatocytes undergo clonal expansion and equally contribute to liver regeneration is not answered by the present study. We observed, when liver disease becomes severe and while the number of DR-derived hepatocytes increases in growing foci, a decline in the total amount of YFP^+ cells owed to a drop in the number of small foci. The absence of mosaicism in DR-derived hepatocyte foci in confetti mice does not support a confluence of growing foci. We therefore suppose that a large proportion of emerging small DR-hepatocytes do not survive in a stressed organ, or are not similarly exposed or do not similarly respond to stimuli enabling them to complete differentiation and to proliferate. A better understanding of the mechanisms supporting DR-derived regeneration is now the next research goal

to identify pathways amenable to therapeutic manipulation for the treatment of liver insufficiency.

BIBLIOGRAPHY

1. Byass P. The global burden of liver disease: a challenge for methods and for public health. BMC Medicine 2014;12:159.

2. European Association for the Study of the Liver. Hepamap: a Roadmap for Hepatology Research in Europe: an Overview for Policy Makers. 2017. Available at: http://www.easl.eu/medias/EASLimg/News/3f9dd90221ef292_file.pdf.

3. Roskams T. Progenitor cell involvement in cirrhotic human liver diseases: From controversy to consensus. Journal of Hepatology 2003;39:431–434.

4. Hul NKM Van, Abarca-Quinones J, Sempoux C, et al. Relation between liver progenitor cell expansion and extracellular matrix deposition in a CDE-induced murine model of chronic liver injury. Hepatology 2009;49:1625–1635.

5. Roskams TA, Theise ND, Balabaud C, et al. Nomenclature of the Finer Branches of the Biliary. Hepatology 2004;39:1739–1745.

6. Kamimoto K, Kaneko K, Kok CYY, et al. Heterogeneity and stochastic growth regulation of biliary epithelial cells dictate dynamic epithelial tissue remodeling. eLife 2016;5:1–26.

7. Roskams T a, Libbrecht L, Desmet VJ. Progenitor cells in diseased human liver. Seminars in liver disease 2003;23:385–396.

8. Stueck AE, Wanless IR. Hepatocyte buds derived from progenitor cells repopulate regions of parenchymal extinction in human cirrhosis. Hepatology 2015;61:1696–1707.

9. Yoon S, Gerasimidou D, Kuwahara R, et al. Epithelial Cell Adhesion Molecule (EpCAM) Marks Hepatocytes Newly Derived from Stem/Progenitor Cells in Humans. Hepatology 2010;53:964–973.

10. Boulter L, Govaere O, Bird TG, et al. Macrophage-derived Wnt opposes Notch signaling to specify hepatic progenitor cell fate in chronic liver disease. Nature medicine 2012;18:572–9.

11. Gouw ASH, Clouston AD, Theise ND. Ductular reactions in human liver: Diversity at the interface. Hepatology 2011;54:1853–1863.

12. Falkowski O, An HJ, Ianus IA, et al. Regeneration of hepatocyte “buds” in cirrhosis from intrabiliary stem cells. Journal of Hepatology 2003;39:357–364.

13. Español-Suñer R, Carpentier R, Hul N Van, et al. Liver progenitor cells yield functional hepatocytes in response to chronic liver injury in mice. Gastroenterology 2012;143:1564–1575.e7.

14. Rodrigo-Torres D, Affo’ S, Coll M, et al. The Biliary Epithelium Gives Rise to Liver Progenitor Cells. Hepatology 2014;60:1367–1377.

15. Jörs S, Jeliazkova P, Ringelhan M, et al. Lineage fate of ductular reactions in liver injury and carcinogenesis. Journal of Clinical Investigation 2015;125:2445–2457.

16. Lu W-Y, Bird TG, Boulter L, et al. Hepatic progenitor cells of biliary origin with liver repopulation capacity. Nature cell biology 2015;17:971–983.

17. He J, Lu H, Zou Q, et al. Regeneration of liver after extreme hepatocyte loss occurs mainly via biliary transdifferentiation in zebrafish. Gastroenterology 2014;146:789–800.e8.

18. Malato Y, Naqvi S, Schürmann N, et al. Fate tracing of mature hepatocytes in mouse liver

homeostasis and regeneration. Journal of Clinical Investigation 2011;121:4850–4860.

19. Schaub JR, Malato Y, Gormond C, et al. Evidence against a stem cell origin of new hepatocytes in a common mouse model of chronic liver injury. Cell Reports 2014;8:933–939.

20. Yanger K, Zong Y, Maggs LR, et al. Robust cellular reprogramming occurs spontaneously during liver regeneration. Genes and Development 2013;27:719–724.

21. Sekiya S, Suzuki A. Hepatocytes, rather than cholangiocytes, can be the major source of primitive ductules in the chronically injured mouse liver. American Journal of Pathology 2014;184:1468–1478.

22. Tarlow BD, Pelz C, Naugler WE, et al. Bipotential adult liver progenitors are derived from chronically injured mature hepatocytes. Cell Stem Cell 2014;15:605–618.

23. Clouston AD, Powell EE, Walsh MJ, et al. Fibrosis correlates with a ductular reaction in hepatitis C: Roles of impaired replication, progenitor cells and steatosis. Hepatology 2005;41:809–818.

24. Raven A, Lu W, Man TY, et al. Cholangiocytes act as facultative liver stem cells during impaired hepatocyte regeneration. Nature 2017;547:350–354.

25. Russell JO, Lu W-Y, Okabe H, et al. Hepatocyte-specific β-catenin deletion during severe liver injury provokes cholangiocytes to differentiate into hepatocytes. Hepatology 2018. Available at: http://doi.wiley.com/10.1002/hep.30270.

26. Deng X, Zhang X, Li W, et al. Chronic Liver Injury Induces Conversion of Biliary Epithelial Cells into Hepatocytes. Cell Stem Cell 2018;23:114–122.e3.

27. Srinivas S, Watanabe T, Lin CS, et al. Cre reporter strains produced by targeted insertion of EYFP and ECFP into the ROSA26 locus. BMC Dev Biol 2001;1:4.

28. Muzumdar MD, Tasic B, Miyamichi K, et al. A Global Double-Fluorescent Cre Reporter Mouse. Genesis 2007;45:418–426.

29. Livet J, Weissman TA, Kang H, et al. Transgenic strategies for combinatorial expression of fluorescent proteins in the nervous system. Nature 2007;450:56–62.

30. Tarlow BD, Finegold MJ, Grompe M. Clonal tracing of Sox9+ liver progenitors in mouse oval cell injury. Hepatology 2014;60:278–289.

31. Mu X, Español-suñer R, Mederacke I, et al. Hepatocellular carcinoma originates from hepatocytes and not from the progenitor / biliary compartment. The Journal of clinical investigation 2015;125:3891–3903.

32. Stradiot L, Verhulst S, Roosens T, et al. Functionality based method for simultaneous isolation of rodent hepatic sinusoidal cells. Biomaterials 2017;139:91–101.

33. Ferreira-Gonzalez S, Lu WY, Raven A, et al. Paracrine cellular senescence exacerbates biliary injury and impairs regeneration. Nature Communications 2018;9:1–15.

34. Pu W, Zhang H, Huang X, et al. Mfsd2a+hepatocytes repopulate the liver during injury and regeneration. Nature Communications 2016;7:1–15.

35. Antoniou A, Raynaud P, Cordi S, et al. Intrahepatic bile ducts develop according to a new mode of tubulogenesis regulated by the transcription factor SOX9. Gastroenterology 2010;136:2325–2333.

36. Jakubowski A, Ambrose C, Parr M, et al. TWEAK induces liver progenitor cell proliferation.

Journal of Clinical Investigation 2005;115:2330–2340.

37. Roskams T, Haele M Van. Hepatic Progenitor Cells: An Update. Clin Liv Dis 2010;46:409–420.

38. Gentric G, Desdouets C. Polyploidization in liver tissue. American Journal of Pathology 2014;184:322–331.

39. Hsu SH, Delgado ER, Otero PA, et al. MicroRNA-122 regulates polyploidization in the murine liver. Hepatology 2016;64:599–615.

40. Gentric G, Maillet V, Paradis V, et al. Oxidative stress promotes pathologic polyploidization in nonalcoholic fatty liver disease. Journal of Clinical Investigation 2015;125:981–992.

41. Firsanov D V., Solovjeva L V., Svetlova MP. H2AX phosphorylation at the sites of DNA double-strand breaks in cultivated mammalian cells and tissues. Clinical Epigenetics 2011;2:283–297.

42. Salleng KJ, Revetta FL, Deane NG, et al. The applicability of a human immunohistochemical panel to mouse models of hepatocellular neoplasia. Comparative Medicine 2015;65:398–408.

43. Tummala KS, Brandt M, Teijeiro A, et al. Hepatocellular Carcinomas Originate Predominantly from Hepatocytes and Benign Lesions from Hepatic Progenitor Cells. Cell Reports 2017;19:584–600.

44. Font-Burgada J, Shalapour S, Ramaswamy S, et al. Hybrid Periportal Hepatocytes Regenerate the Injured Liver without Giving Rise to Cancer. Cell 2015;162:766–779.

45. Li B, Dorrell C, Canaday PS, et al. Adult Mouse Liver Contains Two Distinct Populations of Cholangiocytes. Stem Cell Reports 2017;9:478–489.

46. Huch M, Dorrell C, Boj SF, et al. In vitro expansion of single Lgr5 + liver stem cells induced by Wnt-driven regeneration. Nature 2013;494:247–250.

47. Cao W, Chen K, Bolkestein M, et al. Dynamics of Proliferative and Quiescent Stem Cells in Liver Homeostasis and Injury. Gastroenterology 2017;153:1133–1147.

48. Lin WR, Lim SN, McDonald SAC, et al. The histogenesis of regenerative nodules in human liver cirrhosis. Hepatology 2010;51:1017–1026.

Figure Legends

Figure 1. ***DR cells significantly contribute to the hepatocyte pool during chronic liver injury***

(a) Schematic representation of the experimental design. (b) Liver section obtained from OPN-iCreER^{T2};Rosa26R^{YFP} mice treated for 0 (n=6), 4 (n=2), 6 (n=5), 8 (n=4) and 16 (n=4) weeks CCl_4 stained with Sirius red for collagen. (c) Representative YFP immunohistochemistry on liver sections from OPN-iCreER^{T2};Rosa26R^{YFP} controls (n=6) or mice treated with CCl_4 for 4 (n=2), 6 (n=5), 8 (n=4) and 16 (n=4) weeks. (Scale bar: 100µm) (d) Morphometric quantification of the YFP positive area; (e) Ki67^{+} hepatocyte quantification in control and treated mice. Values are expressed as means of percentage ± SEM; (f) Size of the YFP^{+} patches from the liver sections of OPN-iCreER^{T2};Rosa26R^{YFP} mice treated with CCl_4 for 6, 8 and 16 weeks. (g) Genes involved in senescence and cell cycle arrest pathways were determined by RT qPCR. Values are expressed as mean ± SEM relatively to controls. *p<0,05; ***p<0,001 by 1way ANOVA.

Figure 2. ***DR-derived hepatocytes are fully mature hepatocytes***

Representative pictures of liver sections from TAM-injected-OPN-iCreER^{T2};Rosa26R^{YFP} animals treated with CCl_4 during 8 weeks stained for (a) HNF4α (red)/ YFP (green), (b) Glutamine synthetase GS (red)/YFP (green) and carbamoyl phosphate synthetase CPS1 (red)/YFP (green), (c) Cytochrome P450 2E1 (CYP2E1-red)/YFP (green), (d) carcinoembryonic antigen-related cell adhesion molecule1 (CEACAM1-red)/YFP (green) (scale bars: 50µm). (d) Consecutive sections stained for glycogen (periodic acid-Schiff (PAS) and YFP (brown) (Scale bar: 100µm). (f) Representative pictures of liver sections from TAM-injected OPN-iCreER^{T2};Rosa26R$^{mT/mG}$ mice control (Scale bar: 20µm) and treated for 16 weeks with CCl_4 (Scale bar: 50µm) (g) RNAsequencing data generated heatmap displays similar expression of mature and functional hepatocytic genes.

Figure 3. ***Patches of new hepatocytes with no-hepatocytes origin.***

(a) Representative pictures of liver sections stained with YFP antibody in control mice (n=5) and mice treated with CCl_4 for 6 (n=4) and 8 (n=4) weeks. (b) Representative pictures of liver sections from AAV8-TBG-Cre;Rosa26R^{YFP} animals control and treated with CCl_4 for 6 and 8 weeks stained for HNF4α (red)/ YFP (green)/ck19 (white): in the CTL liver all the hepatocytes are YFP$^+$, expressed HNF4α but not ck19; in CCl_4 livers YFP$^+$ and YFP$^-$ hepatocytes were HNF4α+ ck19-. (c) Size of the YFP- patches from the liver sections of AAV8-TBG-Cre;Rosa26R^{YFP} mice treated with CCl_4 for 6 and 8 weeks.

Figure 4. ***Chronic CCl_4 results in progressive fibrosis and discrete transient accompanying DR***

(a) Liver section obtained from OPN-iCreER^{T2};Rosa26R^{YFP} mice treated for 0 (n=6), 4 (n=2), 6 (n=5), 8 (n=4) and 16 (n=4) weeks CCl_4 stained with cytokeratin 19 (ck19) for bile ducts (arrowhead) and DR (black arrows). (Scale bars: 100µm). **Insert:** higher magnifications of normal bile ducts and DR are shown. (b) Morphometrical quantification of ck19$^+$ cells confirms discrete and transient DR during the progression of the injury. (c) DR markers and (d) genes of the Notch pathway were determined by RT qPCR. Values are expressed as mean ± SEM relatively to controls. *p<0,05; **p<0,01 by 1way ANOVA.

Figure 5. ***Biliary cells in DR and DR-derived hepatocytes undergo clonal expansion.***

Representative confocal pictures of liver sections of OPN-iCreER^{T2};Rosa26R^{Confetti} mice treated with CCl_4 for 8 weeks (n=4) showing (a) DR and (b) and DR-derived hepatocyte patches (scale bar: 20µm). (c) Size in µm^2 (mean ± SEM) of YFP$^+$ and YFP$^-$ hepatocytes in OPN-iCreER^{T2};Rosa26R^{YFP} mice. Quantification of (d) ki67$^+$ and (e) phosphoHistone-H3 (PHH3)$^+$ hepatocytes in YFP$^+$ and YFP$^-$ populations in livers from OPN-iCreER^{T2};Rosa26R-YFP mice treated for 6, 8 and 16 weeks. *p<0,05 **p<0,01 **** p<0,001 by t-test in (c-e)

Figure 6. ***Upon injury, DR-derived hepatocytes face the same DNA-damage level, but better cope with it.***

(a) Gene expression for genes involved in the DNA repair machinery in healthy hepatocytes (white bar), DR-derived hepatocytes (green bar) and native hepatocytes (red bar) sorted from TAM-treated OPN-iCreER^{T2};Rosa26R$^{mT/mG}$ mouse livers after 6 and 8 weeks CCl4. Quantification of (b) γH2AX^{+}/YFP^{+} and γH2AX^{+}/YFP^{-} hepatocytes after 8 weeks CCl_4 (c) apoptotic TUNEL^{+} hepatocytes in YFP^{+} and YFP^{-} populations in livers from OPN-iCreER^{T2};Rosa26R-YFP mice treated for 6, 8 and 16 weeks with CCl_4. (d) Gene Set enrichment analysis in mTomato (RED) native hepatocytes and mGFP (GREEN) DR-derived hepatocytes sorted from TAM-treated OPN-iCreER^{T2};Rosa26R$^{mT/mG}$ mouse livers after 16 weeks of CCl_4 (e) Analysis of nuclear ploidy in OPN-iCreER^{T2};Rosa26R^{YFP} mice treated for 16 weeks with CCl_4 (n=4). Box plot of the percentage of the tetraploid (4n) and highly polyploid (≥8n) nuclei relative to mononuclear polyploid nuclei. *p<0,05 **p<0,01 **** p<0,001 by t-test in Mann-Whitney test.

Figure 7. ***DR-derived hepatocytes have a survival, proliferative and DNA repair advantage upon recovery.***

OPN-iCreER^{T2};Rosa26R^{YFP} mice were treated for 16 weeks with CCl_4 and analysed 72h after last CCl_4 injection (n=4) or after 2 and 4 weeks of CCl_4-free recovery period (n=4 and n=3, respectively). (a) YFP immunohistochemistry (scale bar: 100µm) with (b) morphometric quantification of YFP^{+} area; (c) analysis of the size in the YFP^{+} patches and (d) of the size (in µm^2) of the YFP^{+} and YFP^{-} hepatocytes. (e) Representative picture of liver sections stained for Ki67/YFP. (Scale bar: 50µm). Quantification of the (f) Ki67 index and (g) PHH3 index in YFP^{+} and YFP^{-} hepatocytes**;** (h) Quantification of the γH2AX^{+}/YFP^{+} and γH2AX^{+}/YFP^{-} hepatocytes.*p<0,05, **p<0,01, ****p<0,0001 by 1way ANOVA (b, c, e) or t-test (d, g, h).

Figure 8. ***DR-derived hepatocytes in cirrhotic regenerative nodules.***

(a) Representative liver harvested from OPN-iCreER^{T2};Rosa26R^{YFP} mice treated for 24 weeks with CCl_4 (n=10), (b) YFP immunohistochemistry (bar size: 1mm) with white arrows pointing towards YFP$^-$ nodules, green arrows towards YFP$^+$ nodules, and the white/green arrow towards a mosaic nodule. (c) Percentage of YFP$^+$ and YFP$^-$ nodules per liver section (one dot per liver). (d) Representative pictures of GS and YFP immunostaining on consecutive slides. (e) Analysis of GS expression in YFP$^+$ and YFP$^-$ regenerative nodules and (f) analysis of tetraploid (4n) and highly polyploid (≥8n) nuclei relative to mononuclear polyploid nuclei. (n=3 in CTL group; n=10 in CCl_4 group). (g) IHC score based on GS, β-catenin and Ki67 (see materials and methods) on YFP$^+$ and YFP$^-$ nodules. ***P<0,001 by t test (c) **p<0,01 by Mann- Whitney test (f) and * P<0,05 by Kolmorogov-Smirnov test (g).

ACKNOWLEDGEMENT: Rosa26R-Confetti reporter mice were a kind gift of Prof. Cedric Blanpain (Université Libre de Bruxelles (ULB), Belgium). The authors thank Prof. F. Lemaigre (DDve Institute, UCL, Brussels, Belgium), who generated the OPN-iCreER^{T2} mice and made them available for our studies; N. Feza-Bingi and V. Lebrun (GAEN lab, UCL, Brussels, Belgium) for excellent technical and animal support; D. Brusa from IREC FACS platform and N. Dauguet from De Duve Institute – Flow cytometry and cell sorting platform in Université Catholique de Louvain for excellent technical assistance; D. Tyteca and P. Van Der Smissen (De Duve Institute, UCL, Brussels, Belgium) for assistance with confocal microscopy and Dr E. Danse (Radiology department, St Luc University hospital and UCL, Brussels Belgium) who performed ultrasound examination of the mice; Prof. G. Farrell for discussion and critical comments on the manuscript.

Figure

Click here to download high resolution image

FIGURE 1

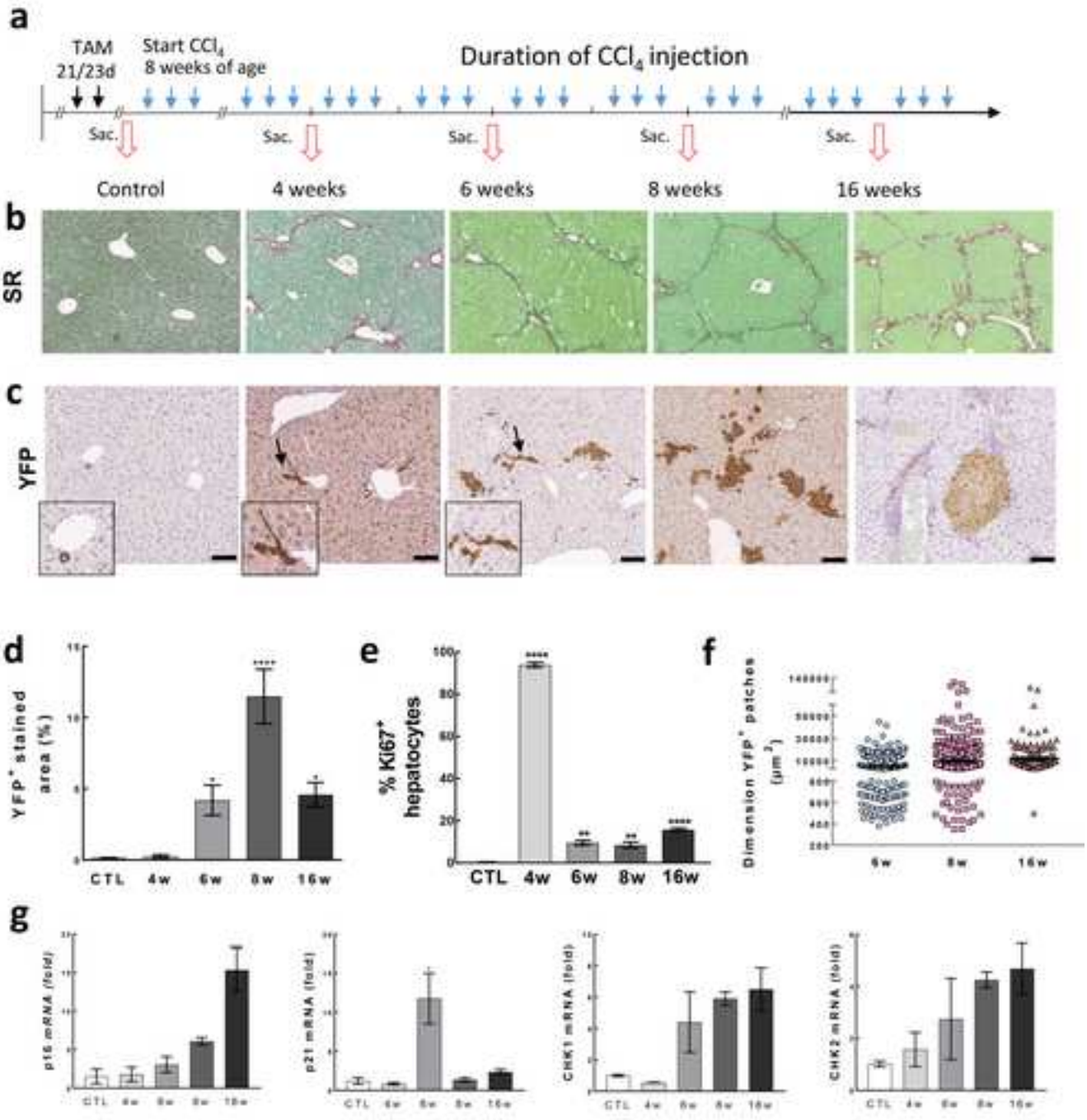

Figure 2

Click here to download high resolution image

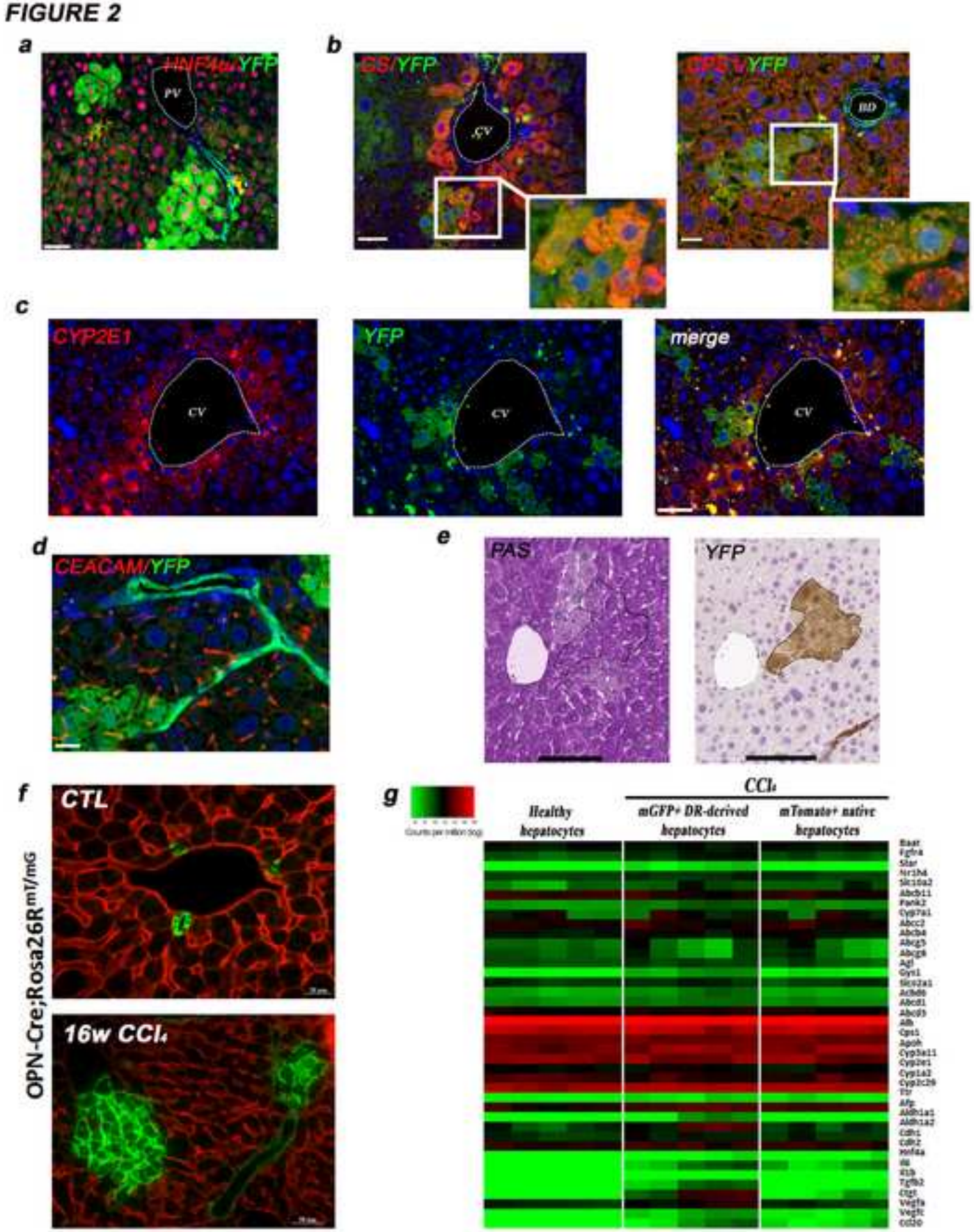

Figure 3

Click here to download high resolution image

FIGURE 3

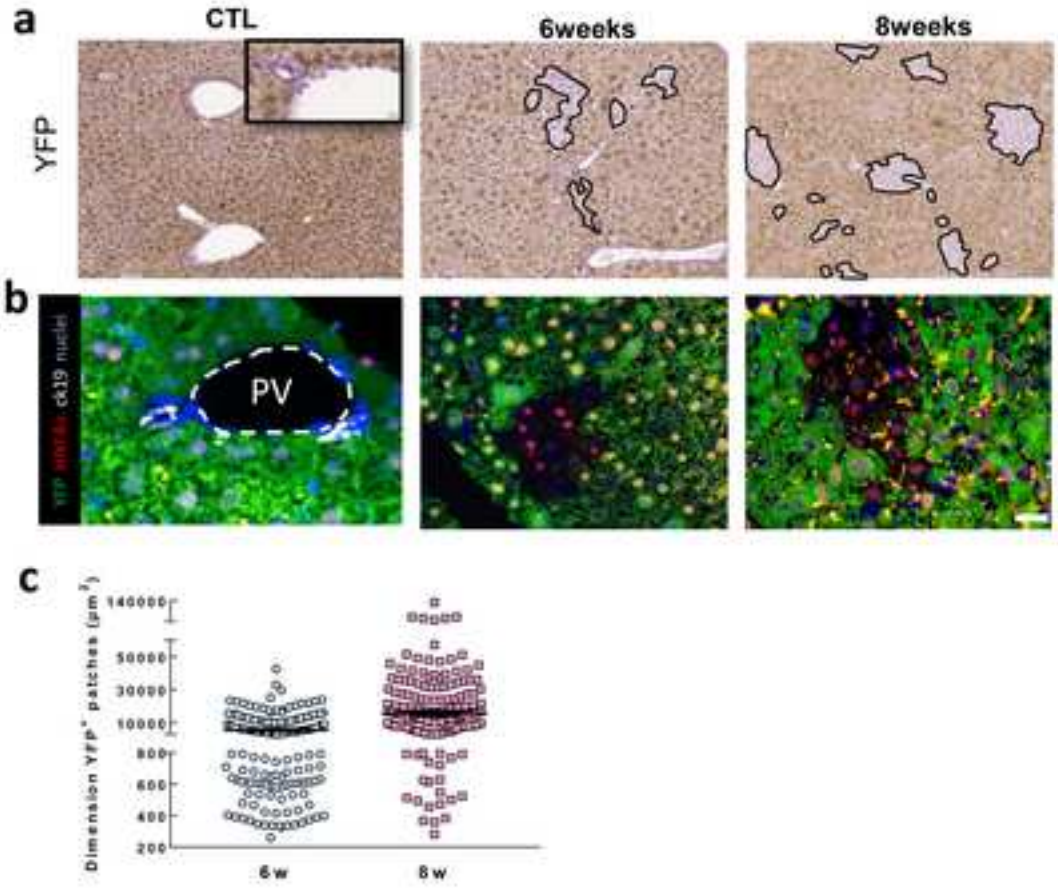

Figure 4

Click here to download high resolution image

FIGURE 4

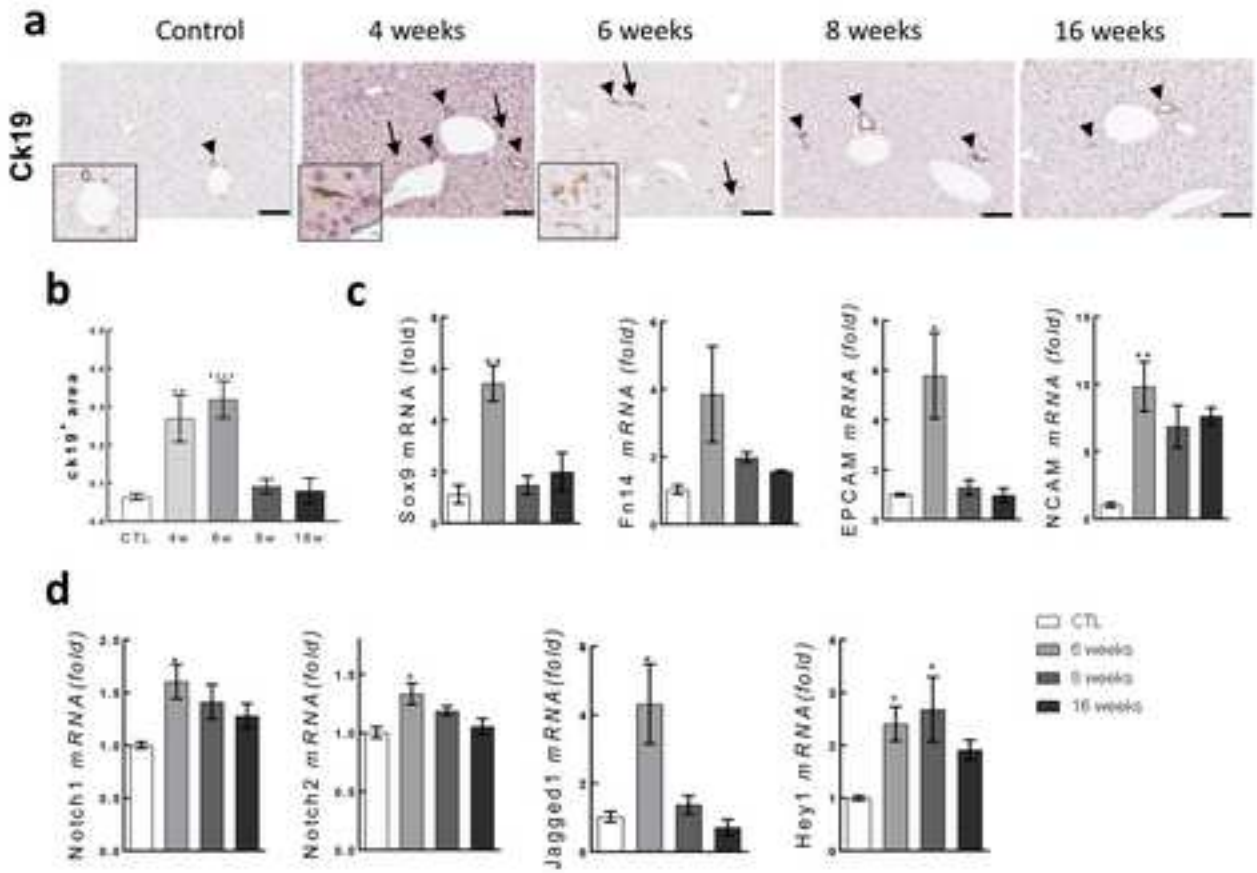

Figure 5

Click here to download high resolution image

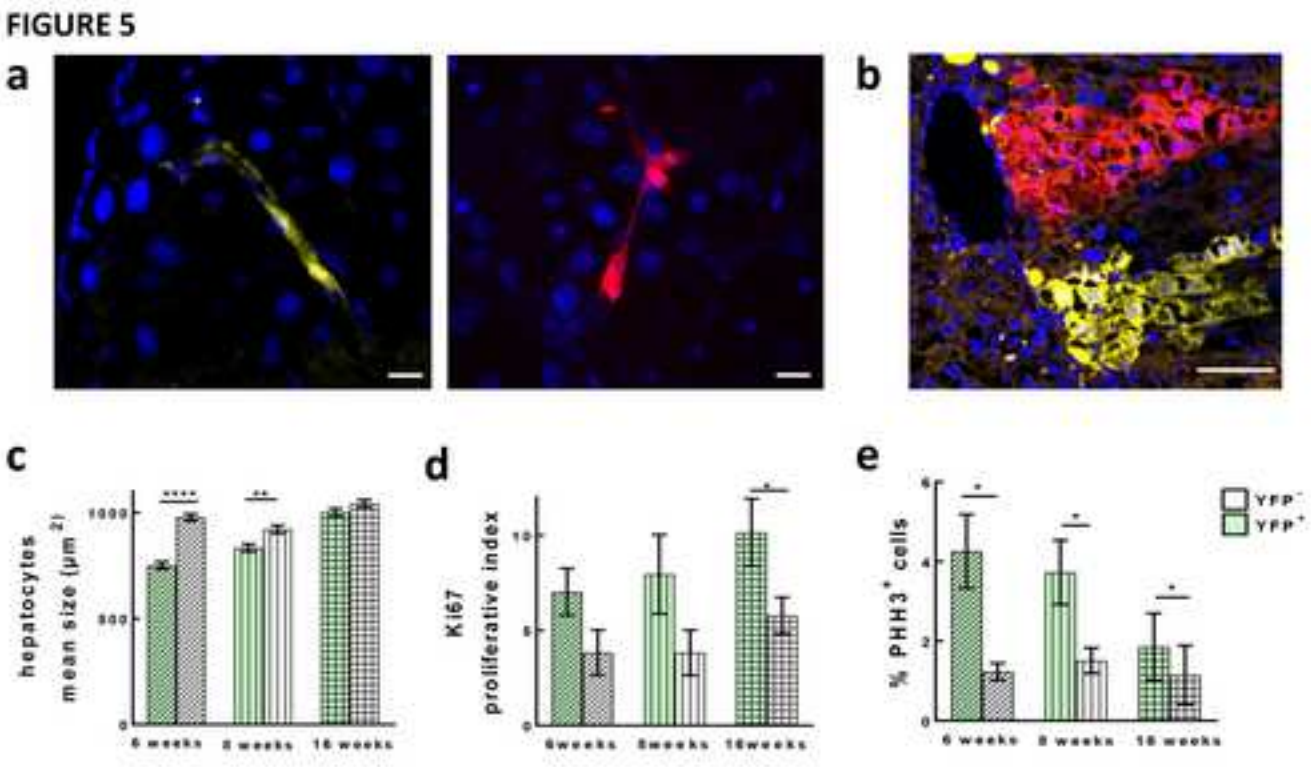

Figure 6

Click here to download high resolution image

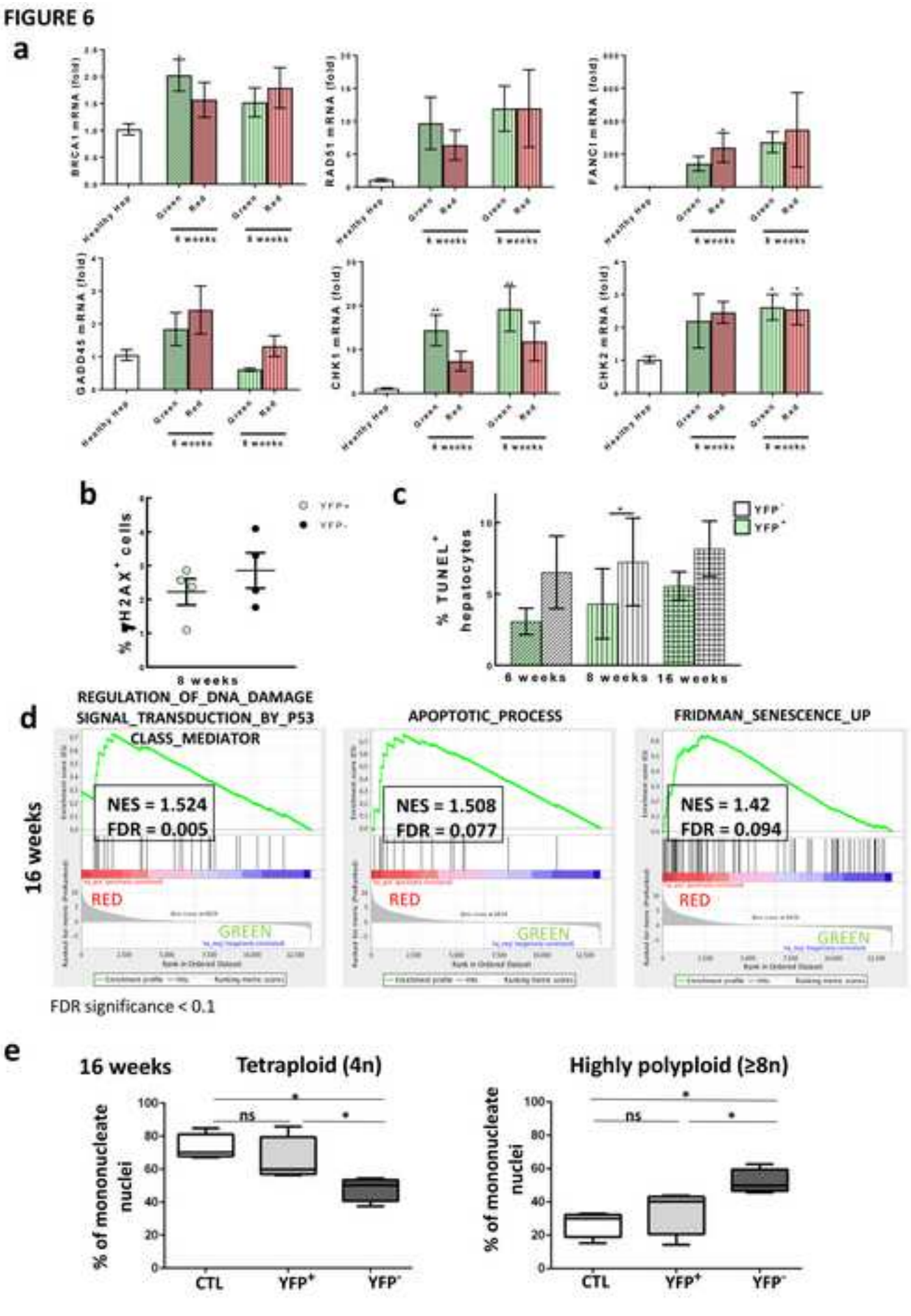

Figure 7
Click here to download high resolution image

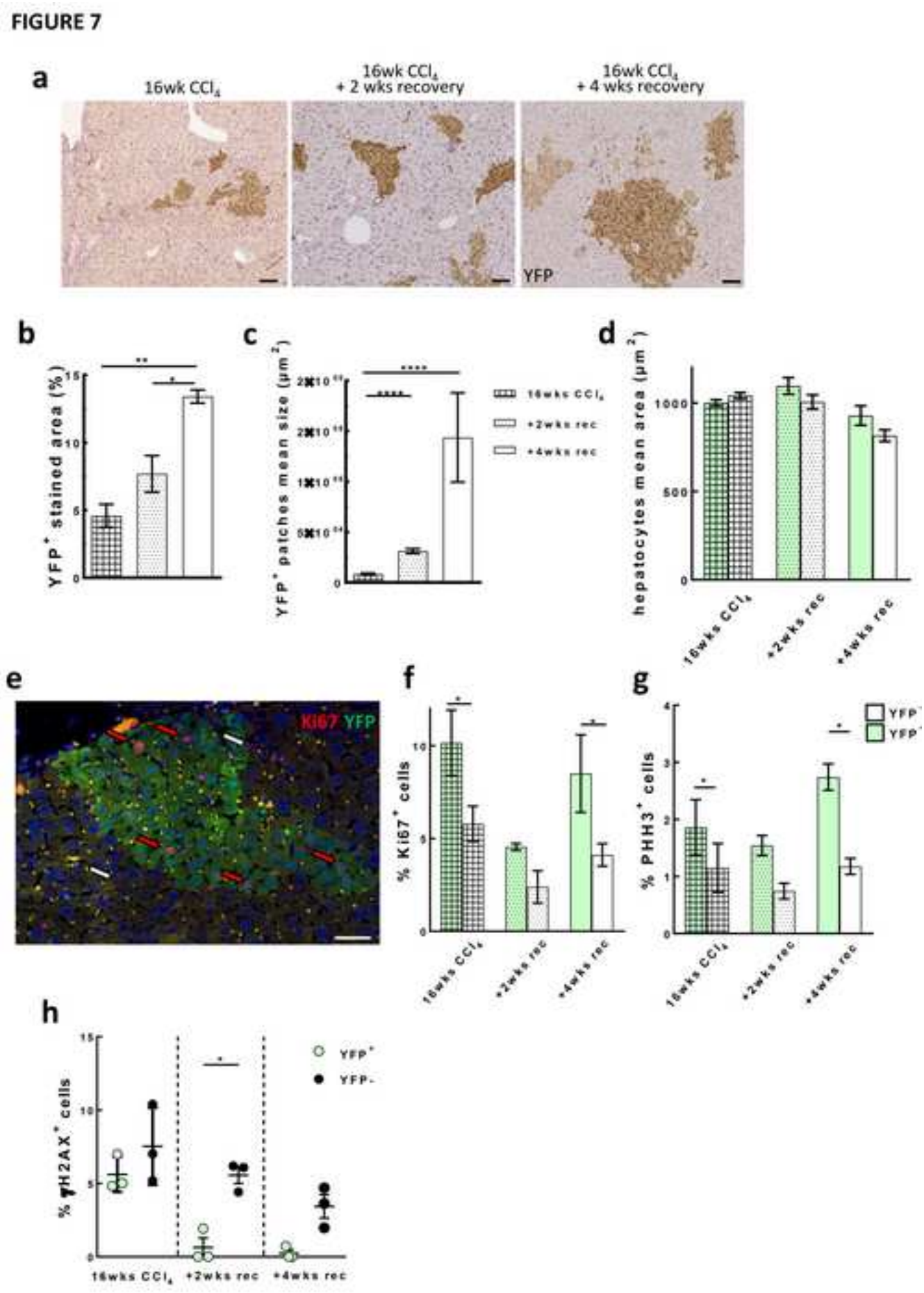

Figure 8

Click here to download high resolution image

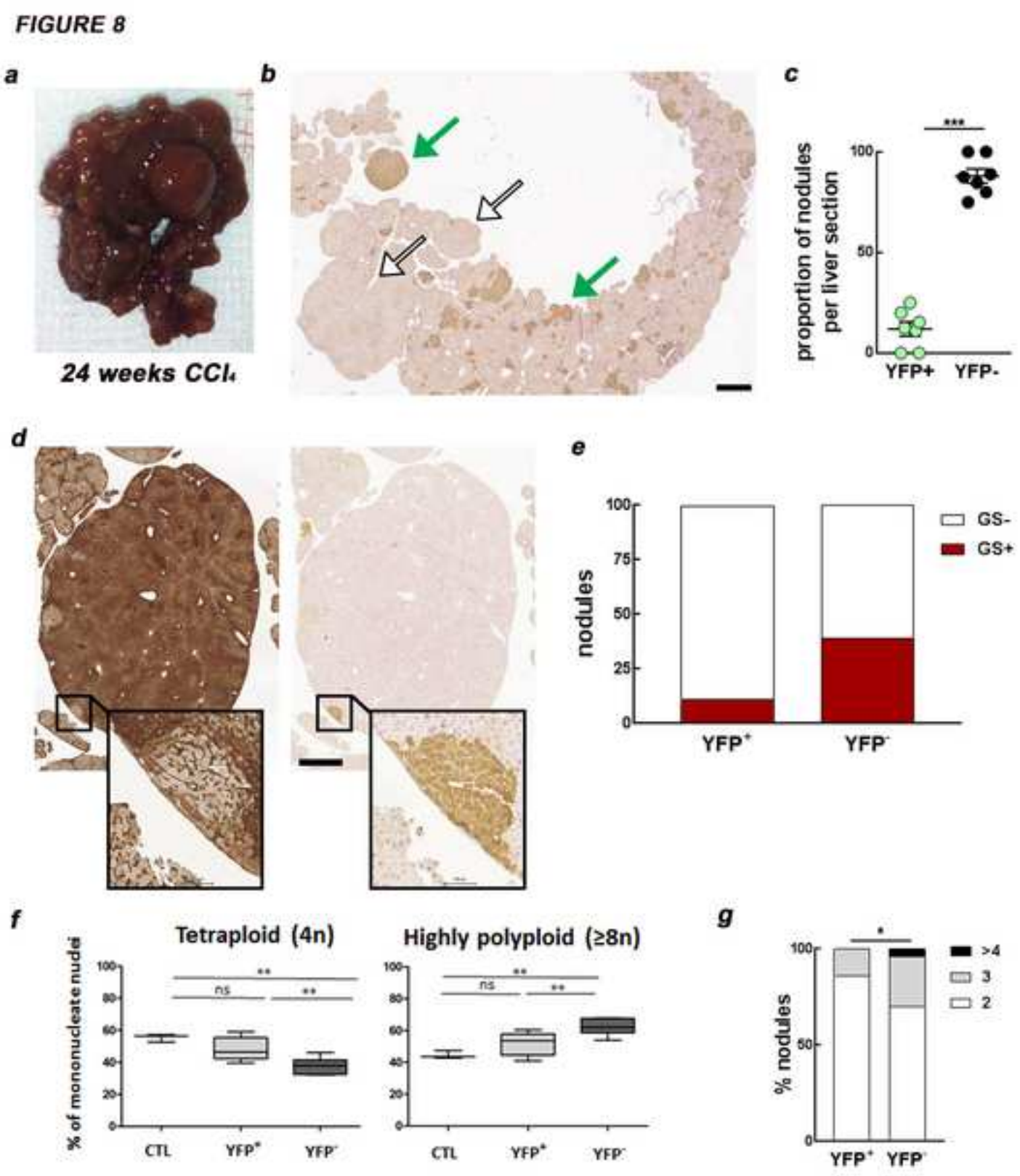

Supplementary material

Click here to download Supplementary material: Suppl. Information.docx

Supplementary material

Click here to download Supplementary material: Supplementary figures.pdf